Cav03-GS-11-004

Fifth International Symposium on Cavitation (CAV2003)
Osaka, Japan, November 1-4, 2003

CAVITATION BUBBLE COLLAPSE AND IMPACT IN THE WAKE OF A CIRCULAR CYLINDER

Yasuhiro Saito
Department of Mechanical Engineering
Kanazawa Institute of Technology, Japan
E-mail: y-sugi@neptune.kanazawa-it.ac.jp

Keiichi Sato
Department of Mechanical Engineering
Kanazawa Institute of Technology, Japan
E-mail: ksato@neptune.kanazawa-it.ac.jp

ABSTRACT

The study for the mechanism of cavitation impulse and erosion has been performed from various kinds of viewpoints. In the present study, a wake-flow field behind a circular cylinder was examined as a representative example of bluff bodies which have a fundamental pattern of separated vortex flow. Cavitation impulses were measured by an accelerometer installed on the outside wall of the test section as well as by the impulsive-force sensor flush-mounted on the inside wall. At the same time, some erosion tests were performed using aluminum plates. Appearances of cavitation bubbles were observed by a still-camera or a high-speed video camera. According to the result, Karman-vortex-like cavities shed downstream are divided into some parts. Then the cavity positioning near the wall collapses rapidly with a colliding motion towards the channel wall. The frequency of cavitation impulses and the distribution of cavitation-damage pits are investigated together with the appearance of bubble collapse. It is found that the number of damage pits is much smaller than the frequency of passing cavities, even on soft aluminum plate.

INTRODUCTION

Cavitation in high-speed liquid flow field is one of the most important problems for fluid machine. It has been studied from various viewpoints on cavitation impact and damage, and much knowledge has been obtained. Cloud cavitation and other various types of vortex cavitation are widely known as cavitation which causes high cavitation impacts [1-5]. We have performed a fundamental research in the flow field around a bluff body and measured high impact in the transition cavitation stage. Collapse behavior of the vortex cavitation bubble near a solid wall was examined in an actual flow field from the viewpoint of the impulsivity that directly connects with the cavitation damage [6-9]. Furthermore, the bubble collapse and the cavitation damage were observed simultaneously, and it was shown that multiple cavitation damage pits could be formed by one cavity collapse [9]. Though, in the experiment, a cavitation impact on the material surface was observed every bubble collapse, it was rare to form a cavitation damage pit.

Knapp [10] investigated the number of bubbles on an aluminum surface with the number of pits around a headform in water, and showed that only one in 30000 traveling cavities produced a damage on the aluminum plate. Hammitt et al. [11] showed that the ratio of the number of bubbles to the cavitation damage pits formed in the mercury by the venturi tube was 10^4. Okada et al. [12] showed that the impacts which produced pits over 4 μm in diameter were about 4 % for impulsive pulses, and the limitative impact load was 9.1 N in the vibratory erosion test for aluminum. However, there seems to be seldom similar researches in vortex cavitation.

In this study, some experimental works are carried out on a shedding type of vortex cavity in the wake of a circular cylinder. This is a fundamental flow field in which the vortex cavitation with high impact appears. In order to solve the problem of cavitation damage mechanism due to vortex cavitation, we focus on the shedding-type vortex cavity and examine the cavity aspects, impacts and damages. And, it is also examined how much the bubble collapse and impact cause cavitation damages.

NOMENCLATURES

Arms : Impulsive acceleration
d : Diameter of circular cylinder
f : Shedding frequency of cavities
fv : Passing frequency of cavities
F : Impulsive force
Fs : Frame speed of high-speed video camera
Np : Number of impulsive pulses
Npit : Number of cavitation damage pits
Re : Reynolds number
P : Static pressure at free stream
Pv : Vapor pressure of water
St : Strouhal number
Tw : Temperature of water
U : Velocity at free-stream
Uc : Contraction velocity at channel
β : Dissolved oxygen content of water
ν : Kinetic viscosity of water
ρ : Density of water
σ : Cavitation number

EXPERIMENTAL APPARATUS AND PROCEDURE

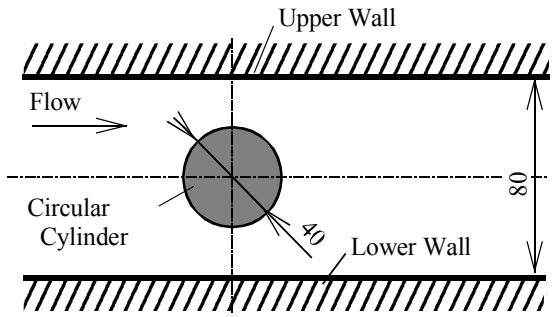

(a) Circular Cylinder Ⅰ

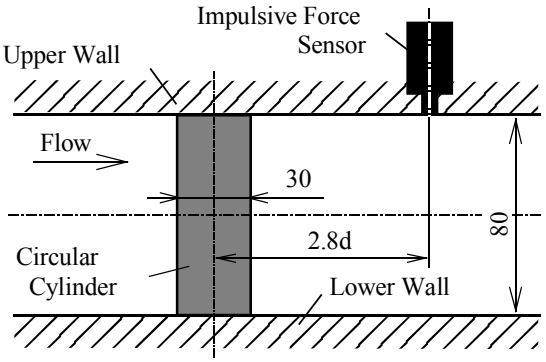

(b) Circular Cylinder Ⅱ

Fig.1 Details of test bodies

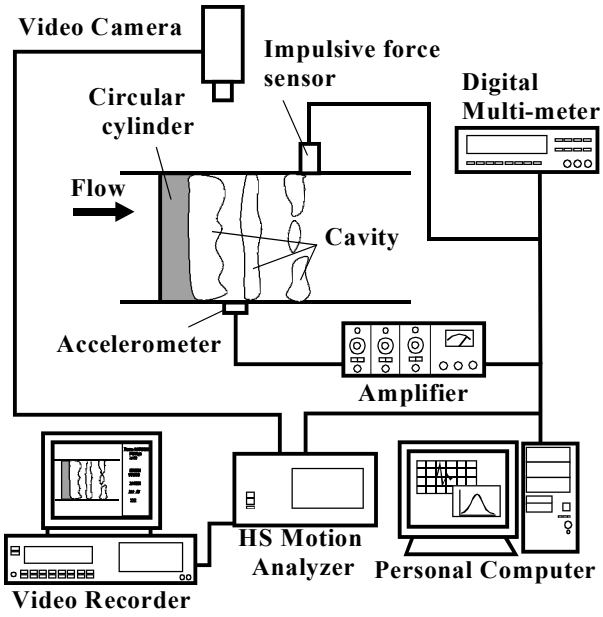

Fig.2 Block diagram of measurement system

The experiment is conducted using a closed-type cavitation tunnel with a rectangular section channel as shown in Fig.1. The test section is 60x80 mm^2 in cross-section. Two types of circular cylinder are used to observe from two directions. The first case, a circular cylinder of d = 40 mm in diameter is installed horizontally in the middle part of the test section as shown in Fig.1 (a). The other case, a cylinder of d = 30 mm in diameter is installed vertically as shown in Fig.1 (b). The blockage ratios are both 0.5. The impact caused by cavitation bubble collapse is measured using two types of sensors. The first one is an accelerometer (TEAC, 501FS/FB) installed on the outside wall of the test section. It is used to measure the impulsive acceleration in cavitation developing process. The other one is PZT sensor [6,7,12] flash-mounted on the inner wall. It is used to measure the cavitation impact directly.

In some case, the sensors are used to make a trigger signal to synchronize the capture of video frame with the cavitation impact. Figure 2 shows the simultaneous measurement system of cavitation impact with its behavior. The system consists of high-speed video camera (Kodak, EXTAPRO model 4540), sensors, digital multi-meter and personal computer. In this system, impulsive pulses due to cavitation bubble collapse are detected by the sensor and conveyed to a personal computer. At the same time, the signal is conveyed to a high-speed video camera as a trigger signal, so that the bubble behaviors and the impulsive pulses can be simultaneously measured.

The experiments are made under constant free-stream velocity by reducing the static pressure in the tunnel. The cavitation number σ, and Reynolds number Re, are defined as follows:

$$\sigma = 2(P-P_v) / \rho U^2 \quad (1)$$

$$Re = U \cdot d / \nu \quad (2)$$

where P and U are static pressure and velocity at free-stream. ρ, Pv and ν are density, vapor pressure and kinetic viscosity of water, respectively. In addition the temperature and dissolved content of oxygen in water are Tw and β, respectively, and Fs is the frame speed of a high-speed video camera.

EXPERIMENTAL RESULTS AND DISCUSSION

Cavitation developing process Figure 3 shows the impulsive acceleration versus cavitation number. The impulsive acceleration was measured by an accelerometer installed on the outside wall. The impulsive acceleration is shown by the rms value of output voltage of the accelerometer. The initiation of cavitation (in this study, the rising point of the impulsive acceleration) occurs in the region of cavitation number σ = 10. And the cavitation shifts to sub-cavitation, transition cavitation and supercavitation with decreasing cavitation number. It is found that the impact increases in transition cavitation stage which shifts from the sub-cavitation stage to the supercavitation stage. In the present case, the peak of the impulsive acceleration appears to be among the cavitation number σ = 4.5 to 5.0.

Figure 4 shows the cavitating-zone length versus cavitation number. This picture was illuminated by the stroboscope of flash period 0.8 μs and flash frequency 20000 rpm and taken by a still camera at shutter speed 1/4 sec. The white part in the pictures shows the cavitating region. With decreasing cavitation number, the cavitating length shows almost the gentle change until near σ=5.5-5.6. The cavitating length rapidly increases, when the cavitation number decreases to less than σ=5.5-5.6. Here, the

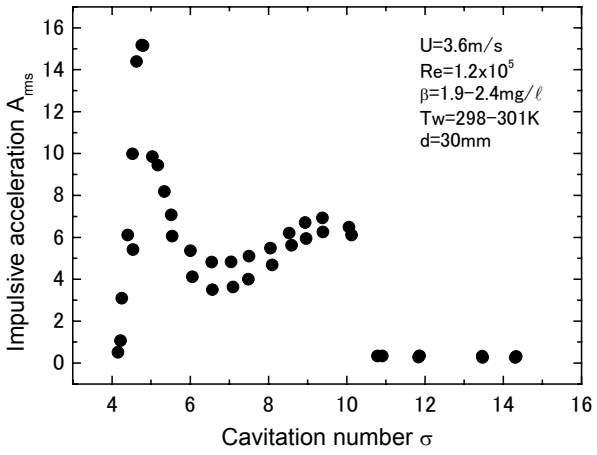

Fig.3 Change of impulsive acceleration in cavitation process

cavitation condition is correspondent to the transition cavitation stage and the impact begins to rapidly increase. It has been confirmed that such phenomenon is also observed in the different flow channel geometry (for example, circular cylindrical orifice flow [13], etc.).

Figure 5 shows the erosion pits distribution after 12 hours test using the aluminum plate (purity: 99.5 %). The test plate was fixed flush with the channel wall and the test was done by keeping cavitation near σ=4.7-4.9 in which the impact became near a peak. The damaged regions can be divided into three parts. The first region (damage region I) is caused by a collapse of vortex cavity near the separated shear layer in the region of near-wake just behind the cylinder. The second region is mainly by cloud cavitation on the about 2.8d downstream of the cylinder center (damage region II). This seems to be correspondent to the first collapse position of the shedding-type cavity. In addition, the region (damage region III) in the downstream seems to be correspondent to the collapse position due to rebounded cavities and bubbles which do not collapse in region II. Many researchers have presented similar results [for example, Mtsudaira et al. [5]]. Though the present result is dominated by the growing condition of cavitation, we choose the condition of cavitation at the impact peak. The impulsive force sensor is flush mounted on the wall surface at 2.8d downstream of the cylinder center and the channel center of region II.

Shedding and collapsing behavior of cavity Figure 6 shows the cavity behavior at impulsive peak. This image was taken by the high-speed video camera system at framing speed of 9000 fps. And Frame No.0 is an image when the impact pulse is detected. The negative and positive number frames correspond to the images before and after the detection of impact, respectively.

It is observed that the cavities are shed periodically. This

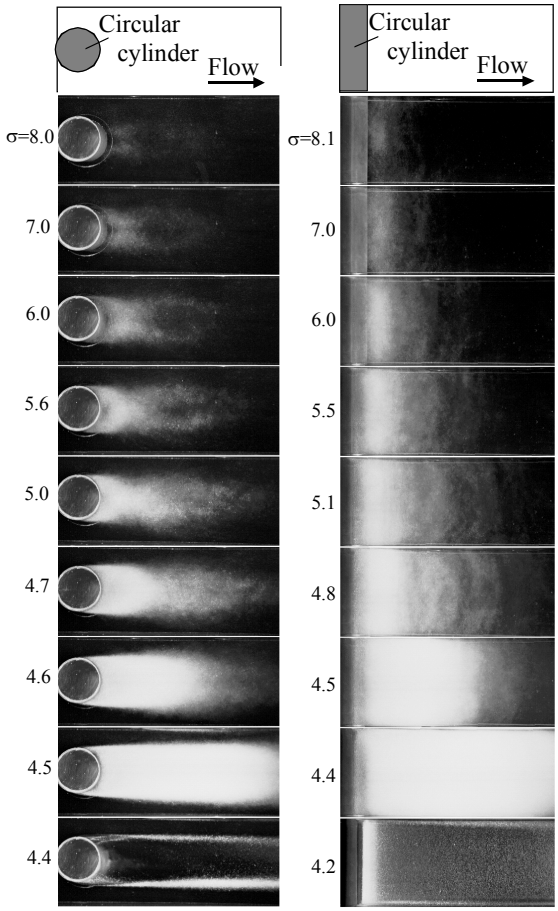

U=2.7m/s
Re=1.1-1.2×10^5
β=1.1-1.5mg/ℓ
Tw=297-300K
d=40 mm
(a)

U=3.6 m/s
Re=1.1-1.2×10^5
β=1.9-2.4 mg/ℓ
Tw=298-301K
d=30 mm
(b)

Fig.4 Time-averaged aspect of cavity

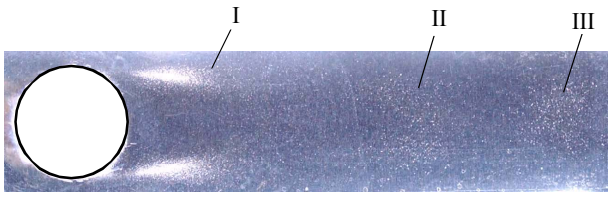

σ=4.9 U=3.6m/s Re=1.1-1.2×10^5 β= 0.8-2.1mg/ℓ
d=30mm t=12hours

Fig.5 Erosion pits distribution

shedding-type cavity is divided into some parts near Frame No.-10 and collapses near the solid wall (Frame No.-8 ～ 0). Especially, the cavity (indicated by the arrow in the figure) remaining near solid wall collapses intensely near the wall and generates high impact.

A sketch of the typical bubble collapse patterns in the wall vicinity is shown in Fig. 7 [Sato et al. 7]. Three types of bubble collapse patterns are also observed in this study. Type A has a collapsing behavior toward the center of bubble at a distance from the solid wall. Type B has a collapsing behavior with an impinging motion to the wall and a part of the bubble attached on the wall surface. Type C keeps a long and slender shape during an almost whole period of the collapsing motion. Especially, it is noticed that Type B corresponds to the axial collapse [3] and relates to the high impact.

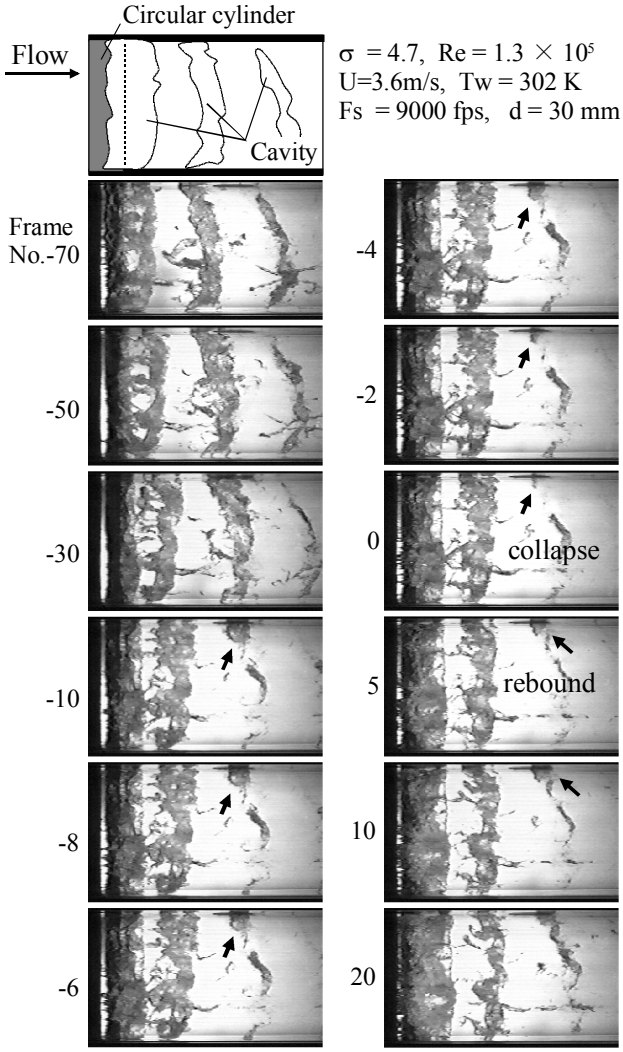

Fig.6 Cavity collapsing behavior in the wake of circular cylinder

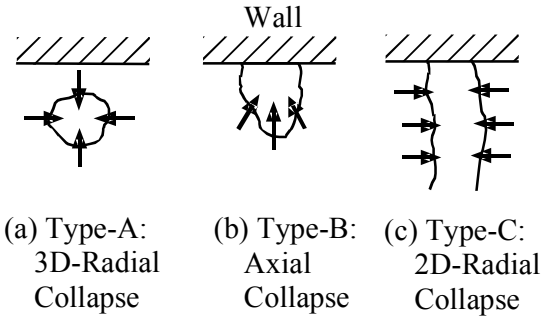

Fig.7 Cavity collapsing patterns[7]

The occurrence frequency of cavity collapse, impact and damage pits The number of vortex cavities was counted in order to examine the frequency of bubble collapses and cavitation damage pits. First, vortex cavities which passed the area of the impulsive force sensor (the position at 2.8d downstream of the cylinder center) were measured in order to be related to the impact generation frequency. The histogram of the passing frequency of cavities fv is shown in Fig. 8. The number of passing cavities is about 100Hz (the shedding frequency of vortex cavities f can be estimated to be about 50Hz, because the vortex cavities in the cylinder wake are alternately shed downstream like the Karman vortex). The strouhal number St is 0.21 in the present experiment. Here, the strouhal number is based on the cavity shedding frequency f, the

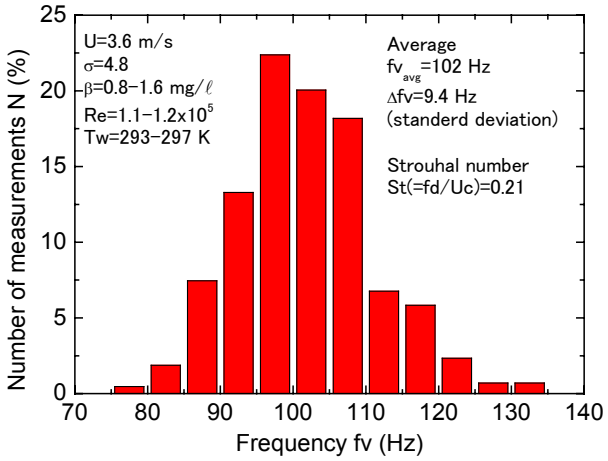

Fig.8 Frequency of passing cavities on impulsive force sensor

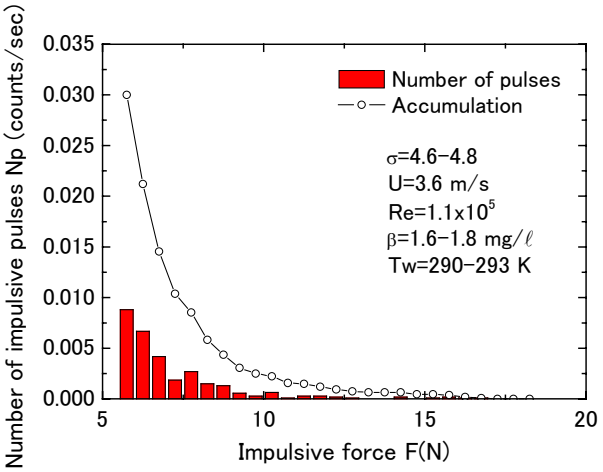

Fig.9 Frequency of impulsive pulses

diameter of the circular cylinder d and contraction velocity Uc at channel. The value agrees with the strouhal number based on the value of vortex shedding frequency under non-cavitation condition.

The occurrence frequency of impulsive pulses detected by the impulsive force sensor was measured. In the measurement, the threshold was established and the pulses of the high impact were counted. Figure 9 shows the number of impulsive pulses generated per unit time Np. As the result, it is found that the frequency of impulsive pulses is large for smaller impacts and the frequency reduces increasing the impact. And, the white round plots in Fig. 9 show the accumulation number of the impacts. It is found that the occurrence number of impacts over 5 N is about 0.03 impacts per second, and it is found to be very small than the vortex-cavity frequency which passes on the impulsive force sensor.

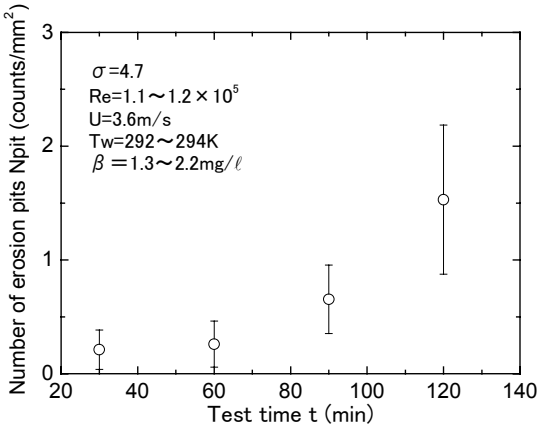

Fig.10 Number of erosion pits against experimental lapse time

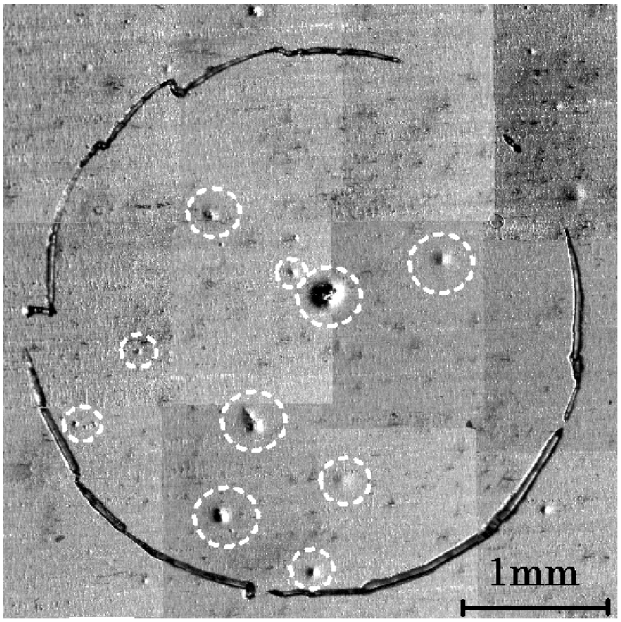

σ=4.7 Re=1.1-1.2x10⁵ U=3.6m/s
Tw=292-294K β=1.3-2.2mg/ℓ t=120 min

Fig.11 Photograph of erosion pits on aluminum plate

Next, it was examined how much cavitation damage pits could be formed at the mounting position of the impulsive force sensor. The aluminum plate was fixed in the sensor mounting position during the erosion test. After that, the aluminum plate surface was observed with the microscope and the cavitation damage pits were counted. The relationship between the cavitation damage pit number Npit and the test duration is shown in Fig. 10. The test region is inside of the 3 mm diameter circle equal to the sensing area of impulsive force sensor. The result of observing the aluminum plate surface after the test (testing time 120 min) by the microscope is shown in Fig. 11. The surface observation was also carried out before the test. The cavitation damage pits over 20 μm are counted. Though pits are not very much formed for about 1 hour after the experiment start, they rapidly increase afterwards. In this case, 10 pits are formed after 120 minutes in the circle of 3mm diameter (part surrounded by the broken line in Fig. 11).

To sum up the above results in this study, the formation frequency of the pits in the sensor area is 10pits/7200sec, that is 0.0014 pits per second. From the accumulation of pulse occurrence frequency as shown in Fig. 9, it is estimated that the damage pit can be formed by large impulsive force over 10 to 15 N. This value is compared with the limitative impulsive force of 9.1 N in an aluminum shown by Okada et al. [12].

The next point is the relationship between the number of passing cavities and damage pits in region II shown in Fig. 5. In region II the number of pits were 10^3 pits. Since the cavity passing frequency is 100Hz, the cavities collapse at 720000 times at least during the testing time. Therefore, in this study, it can be estimated that the ratio of the cavitation damage pits to the number of cavities is the order of about 10^{-3} pits/shed-cavity in case of vortex cavity. This order of value is higher than the result of the erosion test using an aluminum specimen on headform by Knapp [10] as well as the result by Hammitt [11] using a venturi.

CONCLUSIONS

From the viewpoint of vortex cavitation, the bubble collapse aspect, impact and cavitation damage pits (over 20 μm in diameter) were measured in the wake of a circular cylinder.

(1) The passage frequency of the vortex cavity in the test section is about 100 per second in the present experiment. The strouhal number based on the number of shedding vortex cavities agrees approximately with the strouhal number at non-cavitating condition in the wake of the circular cylinder.

(2) As a result of the erosion test using an aluminum plate, the number of cavitation damage pits increases rapidly with elapse of the test time.

(3) The impact necessary to form damage pits for an aluminum plate is about 10 - 15 N on the sensor area in the present experiment.

(4) The occurrence frequency of high impacts causing the cavitation damage pits is much smaller than the number of passing cavities. In this study, the ratio of the number of passing

vortex cavities to the cavitation damage pits on the aluminum plate in damage region II is the order of 10^{-3} pits/shed cavity.

ACKNOWLEDGMENTS

The authors would like to thank Mr. Jun Watanabe and Yoshiyuki Uchiyama who are graduate student, and Hiroyuki Ogawa, Hideki Kaji, Masahiro Sugata, and Motohisa Tsukada who were student of Kanazawa Institute of technology for their considerable assistance. This study was partially funded by the Institute of Nuclei Safety System.

REFERENCES

[1] Selim,S.M.A. and Hutton,S.P., Classification of Cavity Mechanics and Erosion, Proc. I Mech E, Second Int. Symp. on Cavitation, C195/83, (1983), pp. 41-49.

[2] LeCoffre, Y., Marcoz, M. A. and Valibouse, B., Cavitation Erosion in Fluid Systems, ASME, (1981), pp.133-138.

[3] Domingouez-Cortazar, M. A., Franc, J. P. and Michel, J. M., The Erosive Axial Collapse of a Cavitating Vortex: an Experimental Study, Cavitation, IMechE, C453, (1992), pp. 43-48.

[4] Soyama, H., Kato, H. and Oba, R., Cavitation Observations of Severely Erosive Vortex Cavitation Arising in a Centrifugal Pump, Cavitation, Proc. ImechE, C453, (1992), pp.103-110.

[5] Matsudaira, Y., Gomi, Y. and Oba, R., Characteristics of Bubble-Collapse Pressures in a Karman-Vortex Cavity, JSME INT. J., Ser. II, Vol.35, No.2, (1992), pp.179-185.

[6] Sato, K. and Ogawa, N., Collapsing Behavior of Vortex Cavitation Bubble in the Wake of a Circular Cylinder, Cavitation and Gas-Liquid Flow in Fluid Machinery Devices, ASME, FED-226, (1995), pp.119-125.

[7] Sato, K. and Kondo, S., Collapsing Behavior of Vortex Cavitation Bubble Near Solid Wall: Spanwise-View Study, FED-236, Vol.1, (1996), pp.485-490.

[8] Sato, K., Hoshino, K., Kondo, S., and Sugimoto, Y., High-Speed-Video Observations of Vortex Cavitation behind a Cylindrical Bluff-Body: Especially, Bubble Behaviors near Solid Flow Boundary, JSME Centennial Grand Congress, International Conference on Fluid Engineering, Vol. I, (1997), pp. 251-256.

[9] Sato, K., Sugimoto, Y., and Hoshino, K., Bubble Collapsing Behavior and Damage Pits of Separated Vortex Cavitation, Third International Symposium on Cavitation, Grenoble, Vol.2, (1998), pp. 157-162.

[10] Knapp, R. T., Recent Investigation of the Mechanics of Cavitation and Cavitation Damage, Trans. ASME, 77(1955), pp.1045-1054. or Knapp, R. T., Daily, J. W. and Hammitt, F. G., Cavitaion, McGraw-Hill Inc., (1970), pp. 333-335.

[11] Robinson, M. J. and Hammitt, F. G., Detailed Damage Characteristics in a Cavitating Venturi, Trans ASME, J. Basic Eng. Ser. D, 98-1(1967), pp.161-173.

[12] Okada, T., Iwai, Y. and Awazu, K., A study of cavitation bubble collapse pressure erosion, Part 1: method for measurement of collapsing pressures, Wear, Vol.133, (1989), pp.219-232.

[13] Sato, K., and Saito, Y., Unstable Cavitation Behavior in a Circular-Cylindrical Orifice Flow, JSME International Journal Series B, (2002), pp. 638-645.